Numerical application of three-dimensional failure criteria for laminated composite materials

Giovanni Perillo[1] , Nils Petter Vedvik[1] , Andreas T. Echtermeyer[1]

[1]Norwegian University of Science and Technology (NTNU) - Department of Engineering Design and Materials

Abstract: During the last twenty years, composite materials have gained great popularity in many applications such as aerospace, naval and wind turbines. Despite their wide use, the behaviour of composite materials still needs to be thoroughly investigated, especially during and after failure. Only a deep knowledge of these phenomena could maximize the benefit achieved by their use. Many failure criteria have been published in the last thirty years. Among them, the three-dimensional criteria (considering also the out of plane stress) have received particular attention. The three-dimensional failure criteria are used in all cases where the out of plane components of stress are important (impact, bending, etc.). The present work has focused on the implementation of three-dimensional failure criteria (Puck and Hashin 3D) in the commercial Finite Element program ABAQUS, using a USDFLD subroutine. Progressive failure analyses with different material degradation models have been investigated. The numerical analyses have been carried out for laminated composite materials (glass and carbon fibres), modelled using solid elements. Different test cases have been analyzed. The numerical results have been compared with experimental results taken from the literature, showing a satisfactory match. The influences of the failure criteria and material degradation model will be discussed.

Keywords: Composites, Damage, Failure, Progressive Failure Analysis

1. Introduction

In the recent years, composite materials have been increasingly used in many different fields like aerospace, automotive, off shore and many other applications. Composite materials are very attractive for their remarkable strength, stiffeners, weight and for their capacity to be used in particular severe environmental. They can also be designed for specific applications according to the particular load condition, reducing drastically the weight of the components. Despite the wide use of composites in many applications, the non-linear behaviour, during and after partial failure, is still not well investigated. Since most composite materials exhibit brittle failure, without the ductile behaviour of many metals, the non-linear behaviour caused by the failure must be understood and reliable analysis methods need to be used. Composite materials can present different types of local damage: matrix cracking, fibre breakage, fibre/matrix deboning and delamination. The understanding of the initiation and growth of damage is fundamental to predict the real performances of the composite structures under different types of load conditions. This is the main reason to develop advanced failure criteria and particular procedures to follow the damage onset and propagation.

2. Progressive failure analysis

2.1 General overview

In the last thirty years, the progressive failure analysis in laminated composite material have been developed and studied by different authors (Sandhu 1982; Mar 1985; Johnson 1987; Reddy 1992; Tay, Tan et al. 2005; Tay, Tan et al. 2005; Tay, Liu et al. 2006; Tay, Liu et al. 2008).

A typical scheme for the progressive failure analysis is illustrated in Figure 1. The total load δ_{Tot}, applied to the laminated structure, is divided in different sub-steps. For each step, a linear or non-linear analysis is performed until convergence is reached. At the end of each sub-step, stresses and strains are calculated for all the integration points of each element of the model. A global check, using failure criteria, is performed to predict damage initiation. If damage is predicted, the material properties, of the specific integration point, are degraded according to the failure types. At the end of the degradation process, the applied load is incremented according to the general procedure.

A typical progressive failure analysis procedure presents different steps:

- Linear or nonlinear finite elements analysis
- Stress/strain calculations for the different integration points of the model
- The failure criteria check is performed at each integration point to predict the failure
- Local material properties are degraded according to the failure type predicted by the used failure criteria

This research will focus on the last two steps of the progressive failure analysis trying to analyze the influence of different material degradation models and the actual capabilities of the applied three-dimensional failure criteria.

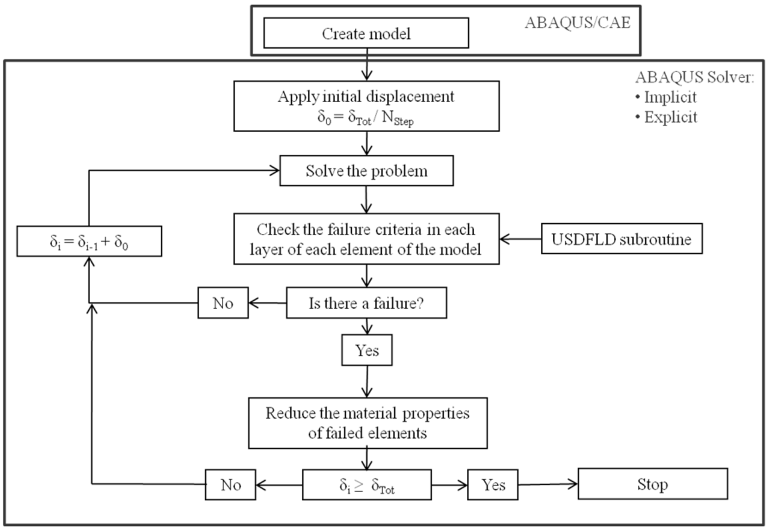

Figure 1: General scheme for progressive failure analysis procedure

2.2 Failure criteria

The ultimate failure of composite structures does generally not occur at the load corresponding to the global first failure. Instead, the final failure is preceded by initial particular damage such as matrix cracking. The damage propagates with increasing load and may change the stress field in the component. This process will typically affect the strength. Laminated composite materials can fail by fibre breaking, matrix cracking or intra-layer delamination. The failure mechanisms depend of the load condition, specimen geometry, material type and staking sequence. In this work, only fibre breaking and matrix cracking are considered.

The onset and the type of the failure can be predicted using different theories published by different authors; a general overview of failure theories is reported in (Orifici, Herszberg et al. 2008). In the last ten years, many "new" criteria have been published thanks to the initiative by (Hinton, Kaddour et al. 2004), different failure theories have been proposed, tested and compared. In the present work, two criteria were selected: the Puck three dimensional criterion (Puck and Schürmann 1998; Puck, Kopp et al. 2001; Puck and Schürmann 2001), has been compared with the classic Hashin three dimensional criterion (Hashin 1980). The two criteria have been chosen for their capability to be used when 3-D out of plane components of the stress are important: for example in impact and bending problems.

2.3 Puck failure criteria

Puck's failure criterion (Puck and Schürmann 1998; Puck, Kopp et al. 2001; Puck and Schürmann 2001) is an interactive stress-based criterion valid for UD (unidirectional) composite lamina (plies).
The Puck criterion is based on a Mohr-Coulomb assumption; the failure is caused by normal and shear stresses (σ_n, τ_{nl} and τ_{nt}) acting on the fracture plane inclined of θ_{fp} to the material plane (see Figure 2). The failure modes that can be predicted by the Puck theory are: the fibre failure ($f_{E(FF)}$) and inter fibre failure ($f_{E(IFF)}$). Inter fibre failure described by Puck is basically matrix cracking. The fibre failure criterion, $f_{E(FF)}$, under a combined load is:

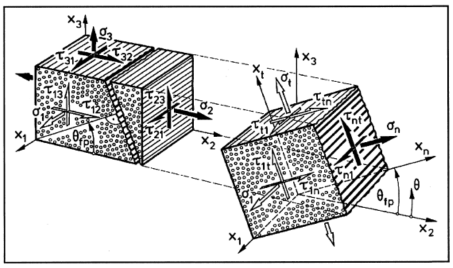

Figure 2: Definition of the fracture plane

$$f_{E(FF)} = \begin{cases} \frac{1}{\varepsilon_{1t}}\left(\varepsilon_1 + \frac{\nu_{f12}}{E_{f1}} m_{\sigma f}\sigma_2\right) & for\ (..) \geq 0 \\ \frac{1}{\varepsilon_{1c}}\left|\left(\varepsilon_1 + \frac{\nu_{f12}}{E_{f1}} m_{\sigma f}\sigma_2\right)\right| & for\ (..) < 0 \end{cases} \quad (1)$$

Where the different parameters mean:

- ε_{1t} and ε_{1c} are the strains to failure in tension and compression respectively.
- E_{f1} and ν_{f12} are the Young modulus and Poisson's ratio for the ply in fibre direction.
- $m_{\sigma f}$ is the 'stress magnification factor' that according to (Puck and Schürmann 1998; Puck, Kopp et al. 2001; Puck and Schürmann 2001), assumes the typical values of 1.3 for glass fibre and 1.1 for carbon fibre composites.

The Puck fibre failure criterion eq. 1 needs particular fibre parameters (E_{f1}, ν_{f12} and $m_{\sigma f}$) that cannot be obtained from standard material testing under uniaxial loads. As presented in the Puck paper (Puck and Schürmann 2001), the results obtained with eq. 1 are comparable to the results obtained with the classical maximum strain criterion (eq. 2). For this reason the maximum strain criterion has been used as fibre failure criterion in this work:

$$f_{E(FF)} = \begin{cases} \frac{\varepsilon_1}{\varepsilon_{1t}} & for\ \varepsilon_1 \geq 0 \\ \frac{\varepsilon_1}{\varepsilon_{1c}} & for\ \varepsilon_1 < 0 \end{cases} \quad (2)$$

For both equations (1) and (2), the fibre fails when the $f_{E(FF)}$ reaches the unit value.

The inter fibre failure criterion, $f_{E(IFF)}$, is based on the assumption that fracture is created only by the stresses that act on the fracture plane. The fracture plane can be inclined with respect to the material plane by an angle (θ) between -90 and +90. The normal and shear stresses acting on this plane are calculated by rotating the three-dimensional stress tensor from the material coordinate system to the fracture plane using the typical tensor transformations:

$$\begin{aligned} \sigma_n(\theta) &= \sigma_2 cos^2(\theta) + \sigma_3 sin^2(\theta) + 2\tau_{23} sin(\theta)\cos(\theta) \\ \tau_{nt}(\theta) &= (\sigma_{3} - \sigma_2) sin(\theta)\cos(\theta) + \tau_{23}\left(cos^2(\theta) - sin^2(\theta)\right) \\ \tau_{nl}(\theta) &= \tau_{31}\, sin(\theta) + \tau_{21}\cos(\theta) \end{aligned} \quad (3)$$

where:

- $\sigma_n(\theta)$ is the stress normal to the fracture plane
- $\tau_{nl}(\theta)$ and $\tau_{nt}(\theta)$ are the shear stresses in the fracture plane, parallel and perpendicular to the fibres direction
- θ is the angle between the fracture plane and the material plane

The inter fibre failure criterion ($f_{E(IFF)}$) is only a function of the stresses acting on the fracture plane:

$$f_{E(FF)} = \begin{cases} \sqrt{\left[\left(\frac{1}{R_\perp} - \frac{P^+_{\perp\psi}}{R_{\perp\psi}}\right)\sigma_n(\theta)\right]^2 + \left(\frac{\tau_{nt}(\theta)}{R_{tt}}\right)^2 + \left(\frac{\tau_{nl}(\theta)}{R_{t\parallel}}\right)^2} + \frac{P^+_{\perp\psi}}{R_{\perp\psi}}\sigma_n(\theta) & for\ \sigma_n \geq 0 \\ \sqrt{\left(\frac{\tau_{nt}(\theta)}{R_{tt}}\right)^2 + \left(\frac{\tau_{nl}(\theta)}{R_{t\parallel}}\right)^2 + \left[\left(\frac{P^-_{\perp\psi}}{R_{\perp\psi}}\right)\sigma_n(\theta)\right]^2} + \frac{P^-_{\perp\psi}}{R_{\perp\psi}}\sigma_n(\theta) & for\ \sigma_n \leq 0 \end{cases} \quad (4)$$

where $R_\perp$ is the failure resistance normal to the fibres, $R_{\perp\psi}$ and $R_{t\parallel}$ are the shear resistances, and $P^+_{\perp\psi}$ and $P^-_{\perp\psi}$ are the slope parameters representing internal friction effects in Mohr-Coulomb failure criterion (more details in (Puck and Schürmann 1998; Puck, Kopp et al. 2001; Puck and Schürmann 2001)). The parameters presented before can be calculated (Puck, Kopp et al. 2001) using:

$$\frac{P_{\perp\psi}^{+}}{R_{\perp\psi}} = \frac{P_{\perp\perp}^{+}}{R_{\perp\perp}}(\cos\psi)^2 + \frac{P_{\perp\parallel}^{+}}{R_{\perp\parallel}}(\sin\psi)^2 \qquad \frac{P_{\perp\psi}^{-}}{R_{\perp\psi}} = \frac{P_{\perp\perp}^{-}}{R_{\perp\perp}}(\cos\psi)^2 + \frac{P_{\perp\parallel}^{-}}{R_{\perp\parallel}}(\sin\psi)^2$$

$$(\cos\psi)^2 = \frac{\tau_{nt}^2(\theta)}{\tau_{nt}^2(\theta) + \tau_{nl}^2(\theta)} \qquad (\sin\psi)^2 = \frac{\tau_{nl}^2(\theta)}{\tau_{nt}^2(\theta) + \tau_{nl}^2(\theta)} \tag{5}$$

$$R_{\perp} = Y_t \qquad R_{\perp\parallel} = S_{21} \qquad R_{\perp\perp} = \frac{Y_c}{2(1 + P_{\perp\perp}^{-})}$$

where Y_t and Y_c are the tension and compression in plane material strength in the direction perpendicular to the fibre.

In addition to the standard material parameters, special Puck parameters are needed. Measuring these parameters required complicated multiaxial testing. However, Puck recommends using the default parameters given in the Table 1:

Table 1: Puck parameters from (Puck, Kopp et al. 2001)

	$P_{\perp\parallel}^{+}$	$P_{\perp\parallel}^{-}$	$P_{\perp\perp}^{+}$	$P_{\perp\perp}^{-}$
Glass fiber	0.30	0.25	0.2 – 0.25	0.2 – 0.25
Carbon fiber	0.35	0.30	0.25 – 0.30	0.25 – 0.30

For all the analysis done in the current work, the maximum value of the Puck parameters (Table 1) have been used. In order to evaluate the inter fibre failure criterion $f_{E(FF)}$, it is required to find the angle of the fracture plane, θ_{fp}, that corresponds to the global maximum of the $f_{E(FF)}$. Due to symmetry, the range of possible angles can be limited to $-90 \leq \theta < +90$. The maximum is found by iteration.

2.4 Hashin 3D failure criteria

The Hashin criterion (Hashin 1980) is also deducted from the Mohr-Coulomb theory, but unlike Puck theory, Hashin didn't take into account the fracture plane. The main reason is that in 1980 it was impossible to get the required computational power to resolve this problem. Hashin's failure criterion considers two different types of fracture for composite materials: fibres and matrix failure. Each of these failure mechanisms should be calculated differently for compression and tension stresses.

The criterion for the fibre failure mechanism is:

$$F_f = \begin{cases} \left(\frac{\sigma_1}{X_t}\right)^2 + \frac{1}{S_{12}{}^2}(\tau_{12}^2 + \tau_{13}^2) & for\ \sigma_1 \geq 0 \\ \left(\frac{\sigma_1}{X_c}\right)^2 & for\ \sigma_1 < 0 \end{cases} \tag{6}$$

Where X_t and X_c are the tension and compression strength in the fibres direction, S_{12} is the in plane shear strength of the layer.

The criterion for the matrix failure mechanism is:

$$F_m = \begin{cases} \frac{(\sigma_2+\sigma_3)^2}{{Y_t}^2} + \frac{\tau_{12}^2-(\sigma_2 \times \sigma_3)}{{S_{23}}^2} + \frac{\tau_{12}^2-\tau_{13}^2}{{S_{13}}^2} & for\ (\sigma_2+\sigma_3) \geq 0 \\ \frac{1}{Y_c}\left[\left(\frac{Y_c}{2\,S_{23}}\right)^2 - 1\right](\sigma_2+\sigma_3) + \frac{1}{4\,{S_{23}}^2}(\sigma_2+\sigma_3)^2 + \frac{1}{{S_{23}}^2}(\tau_{23}^2 - [\sigma_2 \times \sigma_3]) + \frac{1}{{S_{12}}^2}(\tau_{12}^2 + \tau_{13}^2) & for\ (\sigma_2+\sigma_3) < 0 \end{cases} \quad (7)$$

Where $Y_t$and Y_t are the tension and compression strength perpendicular to the fibre direction; S_{13} and S_{23} are the in and out of plane shear strength of the layer. An advantage of the Hashin criterion is that all strength values can be obtained from standard material tests. For both criteria, the failure is predicted when F_f or F_m is equal to the unit value.

2.5 Degradation material models

When the failure is predicted by the failure criteria in a particular position of the composite component, the local properties are reduced according to the failure type predicted by the failure criterion. Many different degradation models have been proposed during the last years (Craddock 1982; Chang, Scott et al. 1984; Gamble, Pilling et al. 1995). In general, degradation material models can be divided, according to (Murray 1990), in three main groups: instantaneous, gradual unloading and constant stress (see Figure 3).

- *Instantaneous:* the material properties are degraded instantaneously to zero, that fit very well the behaviour of brittle materials.
- *Gradual unloading:* the material properties are gradually degraded until zero according to a particular unloading curve.
- *Constant stress:* the material properties are degraded in order to keep constant the local stress.

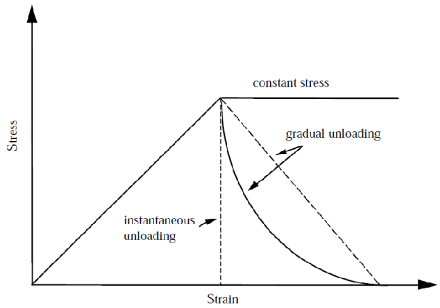

Figure 3: Post failure degradation models

Table 2: Instantaneous degradation material models

		E_{1d}	E_{2d}	E_{3d}	ν_{12d}	ν_{13d}	ν_{23d}	G_{12d}	G_{13d}	G_{23d}	β
Mat. Model 1	Fibre failure	0	0	0	0	0	0	0	0	0	1/100
	Matrix failure DIR:2	E_1	0	E_3	ν_{12}	ν_{13}	0	0	G_{13}	0	
	Matrix failure DIR:3	E_1	E_2	0	ν_{12}	ν_{13}	0	G_{12}	0	0	
	Matrix failure DIR:2+3	E_1	0	0	ν_{12}	ν_{13}	0	0	0	0	
Mat. Model 2	Fibre failure	0	E_2	E_3	0	0	0	0	0	0	1/100
	Matrix failure DIR:2	E_1	0	E_3	0	0	0	0	0	0	
	Matrix failure DIR:3	E_1	E_2	0	0	0	0	0	0	0	
	Matrix failure DIR:2+3	E_1	0	0	0	0	0	0	0	0	
Mat. Model 3	Fibre failure	0	E_2	E_3	0	0	ν_{23}	0	0	G_{23}	1/100
	Matrix failure DIR:2	E_1	0	E_3	0	ν_{13}	0	0	G_{13}	0	
	Matrix failure DIR:3	E_1	E_2	0	ν_{12}	0	0	G_{12}	0	0	
	Matrix failure DIR:2+3	E_1	0	0	0	0	0	0	0	0	

**The value of zero is not the real value used for the finite element analysis*

In the current work, three different instantaneous degradation material models have been used (see Table 2). These degradation material models have been chosen for their correlation with the physical behaviour of the damaged composite material.

In the FE (Finite Elements) programs, for numerical reason the material property cannot be set equal to zero; for this reason, a reduction factor β has been introduced. The degraded material properties (Table 2) are calculated by multiplying the original value with the reduction factor β (as example: $E_{1d} = 0 \rightarrow E_{1d} = \beta E_1$).

2.6 Introduction to finite elements model

The progressive failure analysis methodology described previously, has been implemented in ABAQUS, a complete FE tools. This software has been chosen for its capability of customization given by the use of the subroutines. With the use of the subroutines it is possible to implement procedures and material behaviours that are not available directly in the software.

ABAQUS has a powerful progressive failure analysis directly implemented in it. However, this procedure does not allow the use of different failure criteria. Only the Hashin two-dimensional criterion is used to predict the onset of the damage for fibre reinforced composite materials. For this reason a custom USDFLD subroutine has been written to use the failure criteria described above.

2.7 USDFLD Subroutine

The progressive failure analysis has been implemented in ABAQUS using the subroutine USDFLD, written in FORTRAN. The USDFLD subroutine allows the use of solution dependents material properties for each integration point of the model using field variables. For each integration point and for each step of the analysis, the USDFLD subroutine is evaluated and the chosen failure criterion is calculated; when the failure is predicted, the local material properties, according to the failure type, are degraded by modifying the field variables. Three different field variables have been defined to allow all the possible combinations of failure that can be predicted using Puck or Hashin criteria.

3. Numerical results

The progressive failure methodology described previously, has been implemented in ABAQUS using the USDFLD subroutine. Different test cases have been used to evaluate the performance of the numerical model compared to the experimental results. Two test cases have been presented in this work:

- Rectangular plate under rail shear loading
- Rectangular plate with hole, loaded in tension.

3.1 Test case one: Rail-shear panel

The rail-shear specimens were cross-ply laminated composites tested by Chang and Chen (Chang 1987) and Shahid (Shahid 1993). The specimens were fabricated using a T300/976 graphite-epoxy composite (properties are reported in Table 3), 24 plies with a thickens of 0.13208mm were used with a symmetric layup of $[0_6/90_6]_s$. The specimens were 152.4 mm long and 25.4mm wide (see Figure 4). The specimens were tested by fixing one of the two longer sides and applying the displacement to the other one (see Figure 4).The finite element model has been meshed using C3D8R elements, standard linear solid elements with layer capability and reduced integration available in ABAQUS. Overall, 816 elements have been used in the model. The used mesh has been determined by a simple mesh convergence analysis.

The progressive failure analysis is performed using ABQUS/Standard solver. A displacement of 0.25mm has been applied to the model with a time step of 0.01s (≈100 total steps). The used time step has been chosen to give a good compromise between computational time and accuracy.

Table 3: Properties for T300/976

Material properties		Value (Shahid 1993)
Longitudinal Young's Modulus	E_1	140000 MPa
Transverse Young's Modulus	E_2 , E_3	9700 MPa
Poisson's Ratio	ν_{12}, ν_{13} ,	0.29
	ν_{23}	0.50*[1]
Shear Modulus	G_{12}, G_{13}	5585 MPa
	G_{23}	3300*[2] Mpa
Longitudinal Tensile Strength	X_t	1517 MPa
Longitudinal Compression Strength	X_c	1593 MPa
Transverse Tensile Strength	Y_t ,Z_t	46 MPa
Transverse Compression Strength	Y_c, Z_c	253 MPa
In-Plane Shear Strength	S_{12}, S_{13}, S_{23}	41.4 MPa

**[1]: Not available from (Shahid 1993); common value*
**[2]: Not available from (Shahid 1993); value calculated using the basic conversion formula*

The total reaction forces measured on the fixed side of the model, calculated with both failure criteria (Hashin and Puck), are compared in Table 4 with the experimental result from (Chang 1987). They are also compared in Figure 5 with the analytical calculations from (Shahid 1993). The results presented in Figure 5 show clearly that the predicted ultimate failure of the specimen is not affected by the used failure criteria (Puck and Hashin). Also the different degradation material models do not change the final failure of the specimen; only the post failure behaviours are influenced by the used model. The predicted failure loads are approximately 15% higher than the experimental one measured by (Chang 1987). This similarity of the results, using different failure criteria and degradation material model, is due to the absence of a real progression of the damage in the model under the applied load condition. The complete failure of the specimen happens suddenly without any failure in the previous step, producing a complete reduction of the total strength of the specimen. This behaviour is comparable to the analytical one predicted by (Shahid 1993) and shown in Figure 5.

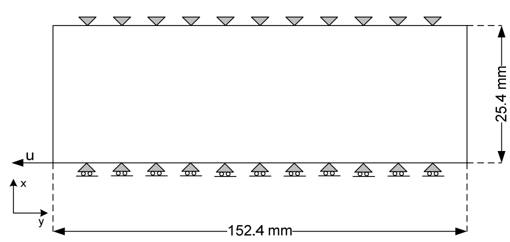

Figure 4: Geometry, loading, and boundary conditions of rail-shear panel

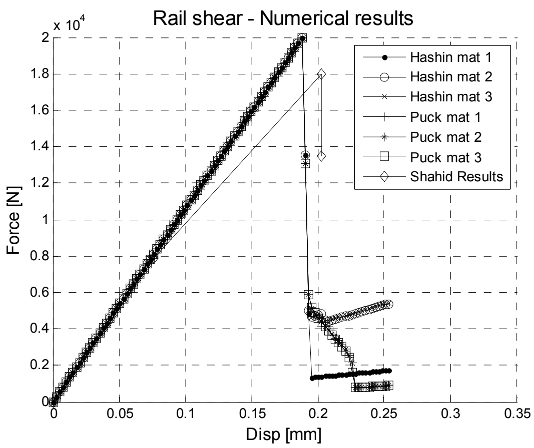

Figure 5: Numerical results for rail-shear panel

It is important to notice the different types of failure predicted by the two failure criteria shown in Figure 6. The Hashin criterion predicts failure near the fixed edge, both fibre and matrix failure at the ultimate load. The predicted failure type, using Puck failure criterion, is completely different, only matrix cracking is present near the upper and lower fixed edge. Despite the differences in the predicted failure types, the ultimate failure loads, with both failure criteria, are the same.

Table 4: Rail-shear panel – Numerical and experimental results

Experimental results (Chang 1987)	Used Failure criteria	Degradation material model					
		Mat1		Mat2		Mat2	
17268 [N]	Hashin	19968	+15 [%]	19970	+15 [%]	19965	+15 [%]
	Puck	19966	+15 [%]	19969	+15 [%]	19966	+15 [%]

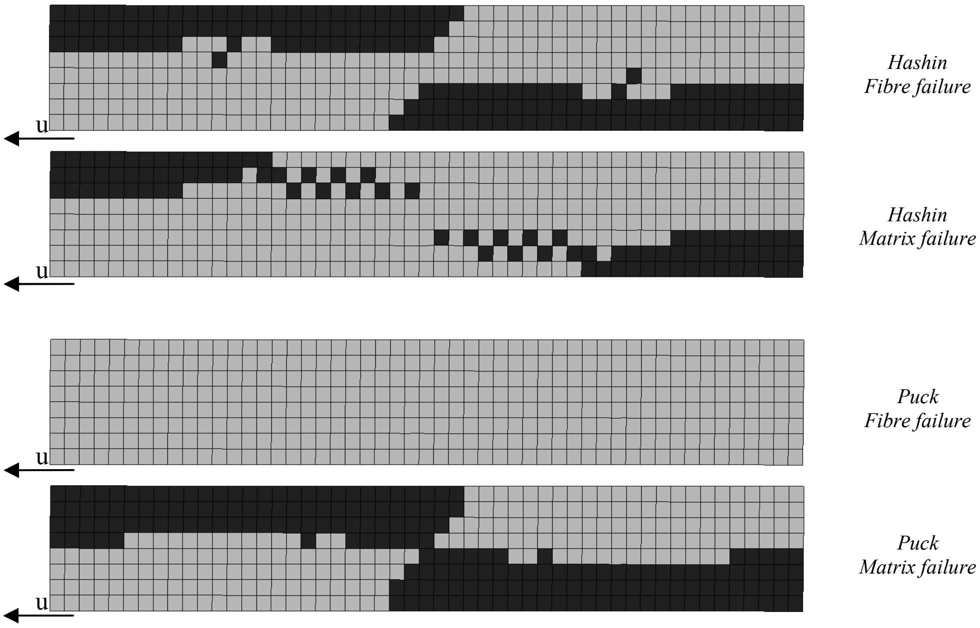

Figure 6: Failure distribution (black) on the specimen at the failure load

3.2 Test case two: Plate with central hole

The numerical results for a rectangular plate with a central hole have been compared with the experimental ones obtained by Tan (Tan 1991) and Chang and Chen (Chang 1987). The dimensions of the specimens are showed in Figure 7.

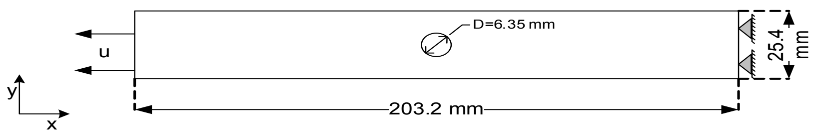

Figure 7: Plate with central hole - Geometry, loading, and boundary conditions

The material used for the specimen is a 20 ply symmetric composite made from T300/1034-C carbon fibres reinforced epoxy with a ply thickness of 0.1308mm. The general ply properties from (Chang 1987; Tan 1991) are reported in the Table 5. Three different symmetric layups were tested: $[0/(\pm45)_3/90_3]_s$, $[0/(\pm45)_2/90_5]_s$ and $[0/(\pm45)/90_7]_s$. The different laminates have the same number of 0° plies but different number of the 90° plies and ±45° plies.

The model has been meshed using 1520 standard linear solid elements with layer capability and reduced integration available in ABAQUS (C3D8R). The model has been meshed to obtain the best accuracy using higher elements density at the hole. The remaining part of the model has been modelled using a coarse mesh with bigger elements, in order to reduce the required computational time. The meshed model is shown in Figure 8. Like in the previous example, simple mesh size convergence studies were carried out, but they are not reported here.

Table 5: Properties for T300/1034-C

Material properties		Value (Chang 1987; Tan 1991)
Longitudinal Young's Modulus	E_1	146800 MPa
Transverse Young's Modulus	E_2 , E_3	11400 MPa
Poisson's Ratio	ν_{12}, ν_{13}	0.30
	ν_{23}	0.50*[1]
Shear Modulus	G_{12}, G_{13}	6100 MPa
	G_{23}	3800*[2] MPa
Longitudinal Tensile Strength	X_t	1730 MPa
Longitudinal Compression Strength	X_c	1379 MPa
Transverse Tensile Strength	Y_t ,Z_t	66.5 MPa
Transverse Compression Strength	Y_c, Z_c	268.2 MPa
In-Plane Shear Strength	G_{12c}, G_{13c}, G_{23c}	58.2 MPa

*[1]: *Not available from (Chang 1987; Tan 1991); common value*

*[2]: *Not available from (Chang 1987; Tan 1991); value calculated using the basic conversion formula*

A total displacement of 2mm has been applied in direction x (horizontal in Figure 7) with a time step of 0.01s (≈100 total steps). A non-linear static analysis has been performed using ABAQUS/Standard. Each model with different layups has been analysed until failure, using the two implemented failure criteria (Hashin and Puck) and the three different degradation material models (Table 2).

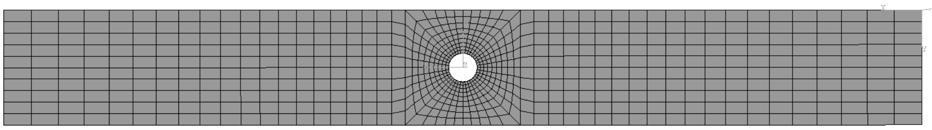

Figure 8: Plate with hole – Meshed model

The results are reported in Figure 9, Figure 10 and in Table 6. As expected, , it is shown in Figure 10 that for both failure criteria the ultimate failure load decreases with the reduction of the ±45° plies and increase of the 90° plies. The behaviour for the failure strains is very different. Using Hashin, the failure strains for the different layup are close, without a marked reduction. With the Puck criterion, the failure strains are reduced when changing the layup (replacing the ±45° plies with 90° plies). Moreover, using both failure criteria (Hashin and Puck), the predicted ultimate failure loads are lower than the experimental ones. Also in this test case, the different degradation material models do not affect the predicted failure load; also the post damage behaviours do not change significantly with the degradation material models. Very small differences are observable after the failure load with the layup $[0/(\pm45)_3/90_3]_s$. In Figure 10, it is shown clearly that the stress-strain relations, using the different failure criteria, are completely different. Using Hashin as failure criterion, there are no variations of the stress-strain curves before the ultimate failure load; the curves are linear until the complete failure. Using Puck as failure criterion the stress-strain curves are different. Before the final failure, the curves present nonlinear parts. This behaviour represents the damage evolution in the model during the increase of the load due to the change of the stresses distribution. Although the damage evolves in the Hashin model before the final failure, the damage development is not recognizable from the stress-strain relation. In Figure 9 the damage distributions, at the predicted failure load, are plotted on the model for both failure criterion. The results show that the complete failure of the specimens occur when the fibre failure in the 0° layer, propagated from the hole, reaches the external edge of the specimen. This behaviour means that the main part of the applied load is supported by the fibres arranged in the load direction. It is also possible to notice a slight antisymmetry of the results. This is most likely due to the presence of the ±45 plies that make the model slightly non symmetric with respect to the central line. The matrix cracking distribution of the model using the two failure criteria is completely different. This behaviour is due to the fact that the Hashin criterion cannot predict the damage in the 90° plies in this particular condition.

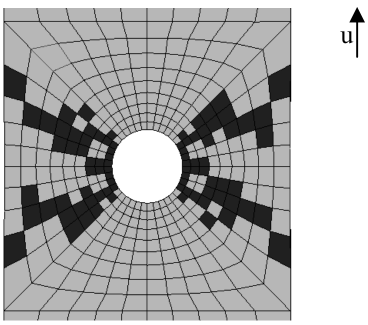

Fibre failure (Black) at maximum load – Hashin

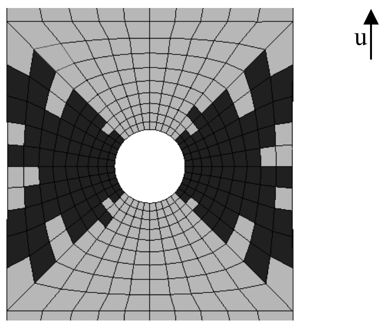

Matrix failure (Black) at maximum load – Hashin

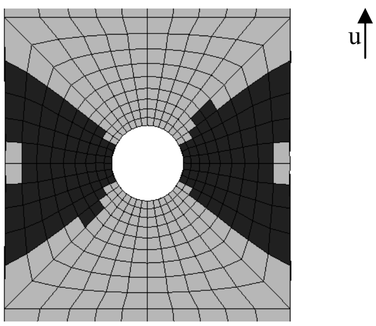

Fibre failure (Black) at maximum load – Puck

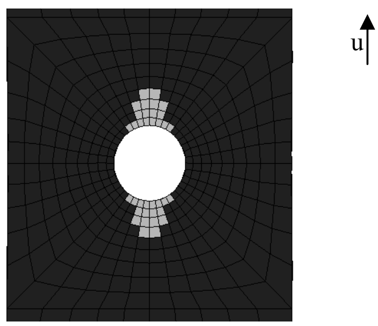

Matrix failure (Black) at maximum load – Puck

Figure 9: Plate with hole – Failure distribution at maximum load (Layup:$[0/(\pm45)_3/90_3]_s$)

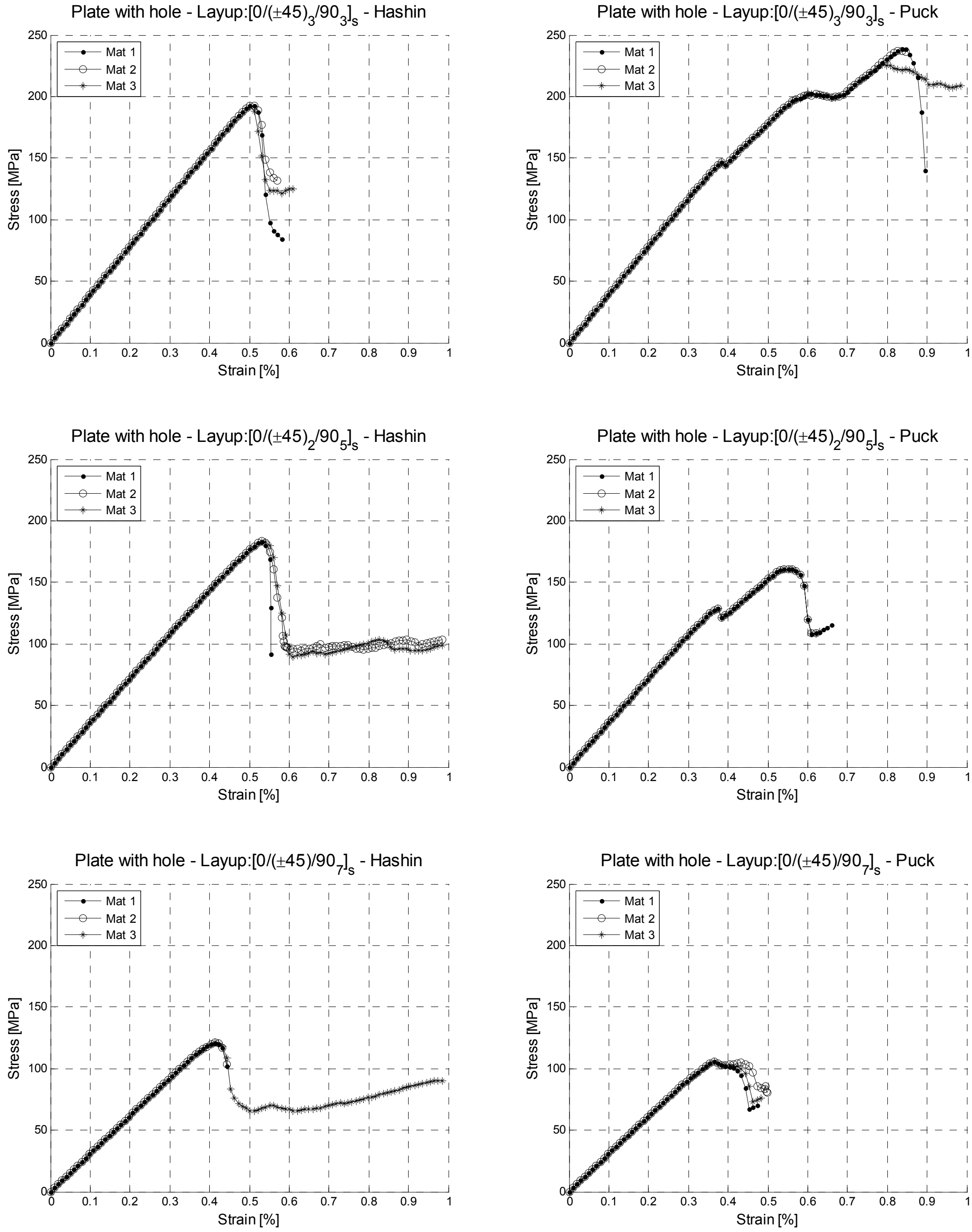

Figure 10: Plate with hole - Numerical results for different degradation material models

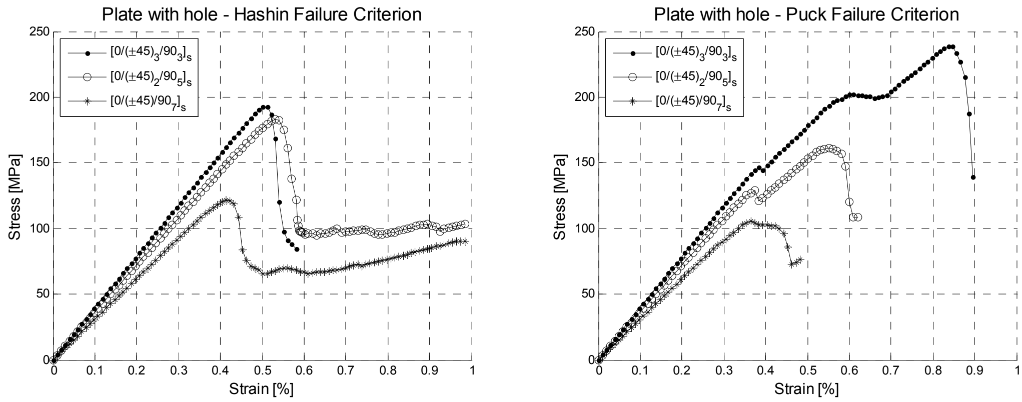

Figure 11: Plate with hole – Numerical results for different layup

Table 6: Plate with hole - Numerical and experimental results

Lay-up	Experimental* From (Tan 1991)	Numerical*											
		Failure criterion: Hashin						Failure criterion: Puck					
		Mat1		Mat2		Mat3		Mat1		Mat2		Mat3	
$[0/(\pm45)_3/90_3]_s$	235,80	192	-18[%]	192	-18[%]	192	-19[%]	239	1[%]	237	0[%]	226	-4[%]
$[0/(\pm45)_2/90_5]_s$	185,80	183	-2[%]	183	-1[%]	183	-1[%]	161	-13[%]	161	-13[%]	161	-13[%]
$[0/(\pm45)/(90)_7]_s$	160,00	120	-25[%]	121	-24[%]	122	-24[%]	105	-34[%]	105	-34[%]	105	-34[%]

**All results are in MPa*

3.3 Conclusion

A first approach to the progressive failure analysis on laminated composite materials with an ad hoc USDFLD subroutine in ABAQUS/Standard has been presented in this paper.

The results show that the Puck and Hashin criteria predict very different damage growth. The Puck failure criterion seems to give better results than Hashin, but only the two test cases presented here are not enough to give the final evaluation. Future work should investigate the capability of the implemented failure criteria to simulate real three-dimensional problems such as impact and bending. The influence of the Puck parameters on the predicted results (final failure and post damage behaviour) has not been analyzed in this paper; the standard values for the carbon fibre materials have been used. Future work should investigate the influence of these parameters on the predicted results. The numerical results presented here are different from the experimental ones (higher for the rail shear and lower for the plate with hole). This behaviour is likely due to the instantaneously degradation type used in the current work. The instantaneously degradation material model does not represent the real behaviour of the composite plies embedded in a laminate. Delamination has also not been modelled directly so far. Future work needs to be done to model and implement the gradual degradation of the material properties using ABAQUS/Standard or ABAQUS/Explicit. In the two test cases different damage distributions have been shown. These results have not been deeply investigated in the current work. Future work should investigate these differences.

A powerful procedure extremely simple to set up has been realized using ABAQUS/Standard. A good compromise between the set up simplicity and results accuracy has been found. A good tool for the initial design of composite materials has been presented here.

4. References

1. "Abaqus Analysis User's Manual."
2. "Abaqus User Subroutines Reference Manual."
3. Chang, F.-K., R. A. Scott, et al. (1984). "Failure of Composite Laminates Containing Pin Loaded Holes—Method of Solution." Journal of Composite Materials 18(3): 255-278.
4. Chang, F. K., and Chang, K. Y (1987). "A Progressive Damage Model for Laminated Composites Containing Stress Concentrations." Journal of Composite Materials Vol. 21: 834-855.
5. Chang, F. K., and Chen, M. H. (1987). "The In Situ Ply Shear Strength Distributions in Graphite/Epoxy Laminated Composites." Journal of Composite Materials 27: 708-733.
6. Craddock, J. N., and Champagne, D. J. (1982). "A Comparison of Failure Criteria for Laminated Composite Materials." Proceedings of the 23rd Structures, Structural Dynamics, and Materials Conference(AIAA Paper 82-0739,): 268-278.
7. Gamble, K., M. Pilling, et al. (1995). "An automated finite element analysis of the initiation and growth of damage in carbonfibre composite materials." Composite Structures 32(1-4): 265-274.
8. Hashin (1980). "Failure criteria for unidirectional composites." J Appl Mech 47: 329-334.
9. Hinton, M. J., A. S. Kaddour, et al. (2004). "Failure Criteria in Fibre-Reinforced-Polymer Composites - The World-Wide Failure Exercise."
10. Johnson, B. (1987). "Elastic-platic stress concentrations around crack.like notches in continuos fiber reinforced metal matrix composites."
11. Mar, D. a. (1985). "Splitting the initiation and propagation in notched unidirectional graphite/epoxy composites under tension-tension cyclic loading."
12. Murray, Y., and Schwer, L. (1990). "Implementation and Verification of Fiber-Composite Damage Models." Failure Criteria and Analysis in Dynamic Response 107(ASME): 21-30.
13. Orifici, A. C., I. Herszberg, et al. (2008). "Review of methodologies for composite material modelling incorporating failure." Composite Structures 86(1-3): 194-210.
14. Puck, A., J. Kopp, et al. (2001). "Guidelines for the determination of the parameters in Puck's action plane strength criterion." Composites Science and Technology 62(3): 371-378.
15. Puck, A. and H. Schürmann (1998). "Failure analysis of FRP laminates by means of physically based phenomenological models." Composites Science and Technology 58(7): 1045-1067.
16. Puck, A. and H. Schürmann (2001). "Failure analysis of FRP laminates by means of physically based phenomenological models." Composites Science and Technology 62(12-13): 1633-1662.
17. Reddy, O. a. (1992). "Finite Element Analysis of Composite Laminates." Kluwer Academic Publishers Dordrecht, The Netherlands.

18. Sandhu, G. a. S. (1982). "Initiation and accumulation of damage in composite laminates."
19. Shahid, I. (1993). " Progressive Failure Analysis of Laminated Composites Subjected to In-Plane Tensile and Shear Loads." Ph. D. Dissertation, Stanford University.
20. Tan, S. C. (1991). "A progressive failure model for composite laminates containing openings." Journal of Composite Materials 25: 556–577.
21. Tay, T. E., G. Liu, et al. (2006). "Damage Progression in Open-hole Tension Laminates by the SIFT-EFM Approach." Journal of Composite Materials 40(11): 971-992.
22. Tay, T. E., G. Liu, et al. (2008). "Progressive Failure Analysis of Composites." Journal of Composite Materials 42(18): 1921-1966.
23. Tay, T. E., S. H. N. Tan, et al. (2005). "Damage progression by the element-failure method (EFM) and strain invariant failure theory (SIFT)." Composites Science and Technology 65(6): 935-944.
24. Tay, T. E., V. B. C. Tan, et al. (2005). "Element-Failure: An Alternative to Material Property Degradation Method for Progressive Damage in Composite Structures." Journal of Composite Materials 39(18): 1659-1675.

5. Acknowledgements

This work was done within the research project COMPACT. The authors would like to thank for the cooperation with Sintef, Flowtite, Nammo and Ragasco, and for the support by the Norwegian Research Council.